Extending the Radiosity Method to Include Specularly Reflecting and Translucent Materials

HOLLY E. RUSHMEIER and KENNETH E. TORRANCE
Cornell University

An extension of the radiosity method is presented that rigorously accounts for the presence of a small number of specularly reflecting surfaces in an otherwise diffuse scene, and for the presence of a small number of specular or ideal diffuse transmitters. The relationship between the extended method and earlier radiosity and ray-tracing methods is outlined. It is shown that all three methods are based on the same general equation of radiative transfer. A simple superposition of the earlier radiosity and ray-tracing methods in order to account for specular behavior is shown to be physically inconsistent, as the methods are based on different assumptions. Specular behavior is correctly included in the present method. The extended radiosity method and example images are presented.

Categories and Subject Descriptors: I.3.3 [**Computer Graphics**]: Picture/Image Generation; I.3.7 [**Computer Graphics**]: Three-Dimensional Graphics and Realism

General Terms: Algorithms

Additional Key Words and Phrases: Backward form factor, forward form factor, global illumination, image synthesis, radiosity, ray tracing

1. INTRODUCTION

A two-pass method that combines the radiosity and ray-tracing approaches to illumination calculations has recently been introduced by Wallace, Cohen, and Greenberg [13] for the generation of realistic synthetic images. The method consists of a first pass, which is an extended radiosity method due to Rushmeier [11], and a second pass, which is a modified form of the distributed ray-tracing technique introduced by Cook, Porter, and Carpenter [2]. Wallace et al. presented a practical application of the two-pass method. The present paper, based on [11], provides the theory and implementation of the first pass, the *extended radiosity method.* The extended radiosity method accounts for specular and ideal diffuse

We acknowledge the support of the National Science Foundation under grants DCR 8203979 and MEA 8401489, the Digital Equipment Corporation via a research grant in computer graphics, the Education Foundation of the American Association of University Women, and the U.S. Army Research Office through the Mathematical Sciences Institute of Cornell University.
Authors' present addresses: H. E. Rushmeier, The George W. Woodruff School of Mechanical Engineering, Georgia Institute of Technology, Atlanta, GA 30332; and K. E. Torrance, Sibley School of Mechanical and Aerospace Engineering, Upson Hall, Cornell University, Ithaca, NY 14853.

Nomenclature list

A	Area
B	Radiosity
$F_{b,nmp}$	Backward mirror form factor
$F_{f,nmp}$	Forward mirror form factor
F_{nm}	Forward diffuse form factor
I	Intensity
L	Number of light sources
N	Number of surfaces
q	Energy flux density
$T_{b,nmp}$	Backward window form factor
$T_{f,nmp}$	Forward window form factor
T_{nm}	Backward diffuse form factor
$\mathbf{V}$	Visibility function
x	Cartesian coordinate
α	Absorptance
ρ	Reflectance
θ	Polar angle
τ	Transmittance
ϕ	Azimuthal angle
ω	Solid angle

Subscripts

abs	Absorbed
b	Back of surface
bd	Bidirectional
d	Diffuse
dh	Directional hemispherical
e	Emitted
f	Front of surface
i	Incident
l	Particular light source l
m	Particular surface m
n	Particular surface n
o	Outgoing
p	Particular surface p
r	Reflected
s	Specular
t	Transmitted

Superscripts

$'$	Virtual point or surface

Other

Underscore indicates vector quantity.

n(t)	indicates the surface intersected by a ray specularly transmitted through surface n.
n(s)	indicates the surface intersected by a ray specularly reflected against surface n.

reflection from surfaces, and specular and ideal diffuse transmission through translucent materials. The relationship of earlier radiosity and ray-tracing methods to the extended method is also reviewed.

The generation of realistic images requires modeling global illumination effects. Ray tracing was introduced by Whitted [14] to account for multiple specular reflections in an environment. Radiosity methods, based on concepts from radiative heat transfer, were independently developed by Goral et al. [6], and by Nishita and Nakamae [9, 10] to account for multiple diffuse interreflections. Recognizing that a complete illumination model must account for all types of interreflection, Kajiya [8] and Immel, Cohen, and Greenberg [7] independently introduced methods to solve the general equation of radiative transfer, with no theoretical restrictions on the type of reflection. The general methods are extremely expensive computationally. Kajiya's Monte Carlo method is basically a ray-tracing method and can be efficient in environments in which directional reflection is important. For diffuse surfaces, however, particularly those that do not have a direct view of a light source, large numbers of rays need to be cast at each pixel to converge to a solution. Immel's method is a type of radiosity method, in which a very large set of simultaneous equations is formed to solve for the intensities from all surfaces in an environment in all directions. Immel's method can be efficient for environments consisting of nearly diffuse surfaces, but the number of equations becomes unmanageable for nearly specular surfaces.

Wallace et al.'s two-pass method was introduced as a practical alternative to the methods of Kajiya and Immel et al. In the first pass, an augmented set of form factors is found to account for the important specular reflections that may affect the intensity of diffuse surfaces. In the second pass, a method of ray tracing for specular reflections is used. This paper provides the underlying theoretical framework for the first step in Wallace et al.'s method. Such a framework is needed to understand the limitations and possible future developments of the two-pass method.

The extended method will be derived by starting with the general equation of radiative transfer. The approach will employ terminology commonly used in radiative heat transfer [12] and optics [3]. Also beginning with the general equation of transfer, the radiosity and ray-tracing methods will be derived. Kajiya has previously outlined the relationship between computer graphics lighting models and a general equation of transfer [8]. The present derivation illustrates the assumptions needed to produce the extended radiosity method. Finally, a series of images illustrates the capabilities of the extended radiosity method.

2. GOVERNING EQUATIONS

Light intensities within a scene are governed by the principles of radiative transfer, and a physically correct lighting model must be based on those principles. An enclosure as shown in Figure 1a will be considered. In this section, all surfaces in the enclosure are allowed to have arbitrary directional and spectral radiation properties for the emission, reflection, absorption, and transmission of light energy (radiation). The material filling the space between the surfaces (the atmosphere) is assumed to be transparent (i.e., radiatively nonparticipating). Furthermore, it will be assumed that light energy is not transferred from one wavelength to another by the aforementioned processes. Thus, each wavelength, or wavelength interval, is independent of all others. With the above assumptions, a general equation governing radiative transport can be developed (i.e., eq. (10)).

2.1 Light Energy

Light is electromagnetic energy and can be expressed as an energy flux density, q, in units of energy per unit area and time. When q represents the total energy flux density leaving a surface (e.g., by emission, reflection, and transmission), it is referred to as the radiosity, B, of the surface.

To account for the directional character of light energy, it is necessary to introduce the radiant intensity I. With angles as defined in Figure 1b, the intensity leaving a surface element dA in a direction (θ, ϕ) is given by

$$I(\theta, \phi) = \frac{dq(\theta, \phi)}{\cos \theta \, d\omega}, \tag{1}$$

where $dq(\theta, \phi)$ is the differential energy flux density leaving the surface within a small solid angle $d\omega$ in the given direction. Intensity is found by expressing dq per unit projected area (thus introducing $\cos \theta$) and by dividing by $d\omega$.

For synthetic image generation, intensity is the appropriate quantity with which to work. The energy flux density reaching the eye from a surface in a scene

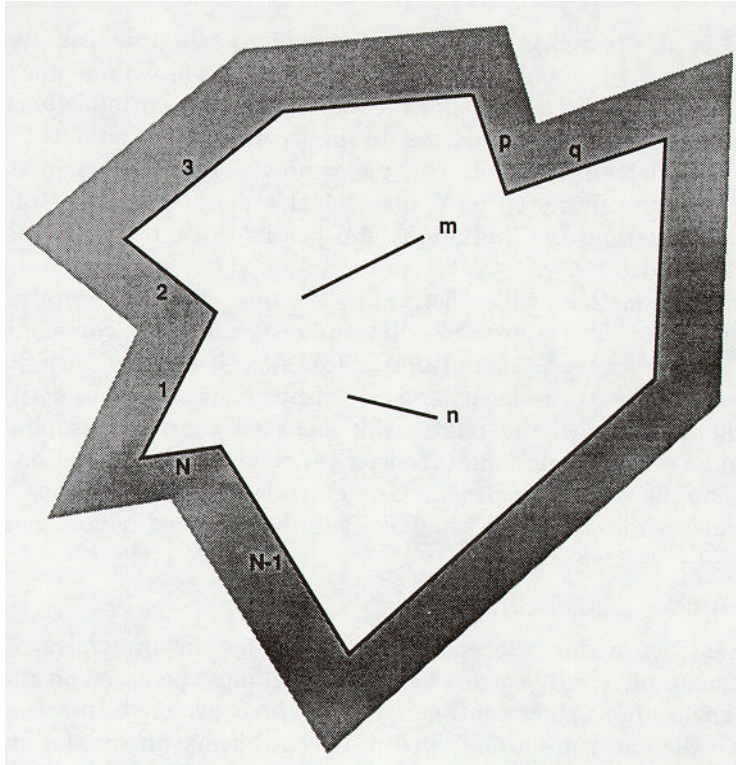

Fig. 1a. Enclosure consisting of N surfaces. The surfaces can emit, reflect, absorb, or transmit light energy, and have arbitrary directional and spectral characteristics.

varies with distance according to an inverse square law. Similarly, the solid angle subtended by a surface as viewed by the eye also varies according to an inverse square law. The intensity, or brightness, perceived by the eye is proportional to the ratio of these two quantities. Thus, from eq. (1), the intensity of a surface in a scene remains constant to an observer as the observer moves toward or away from a scene.

2.2 Interactions of Light with Surfaces

Light is assumed to be emitted, reflected, absorbed, or transmitted only at surfaces within an environment. In an environment, every object will be represented by a set of bounding surfaces. Bounding surfaces may be either opaque or transmitting.

To construct a synthetic image of a scene, it is necessary to know the intensity of light leaving a surface in a scene. As sketched in Figure 1c, this is an intensity function of the form $I_{o,n}(\underline{x}_n, \underline{\theta}_{o,n})$, where o denotes the outgoing intensity, n denotes the particular surface n, $\underline{x}_n$ is a vector to a point on the surface from a coordinate system based on n, and $\underline{\theta}_{o,n}$ denotes a unit vector in the direction $(\theta_{o,n}, \phi_{o,n})$ leaving surface n, referenced to the coordinate system based on n and the local surface normal. The intensity $I_{o,n}$ is composed of emitted, reflected, and

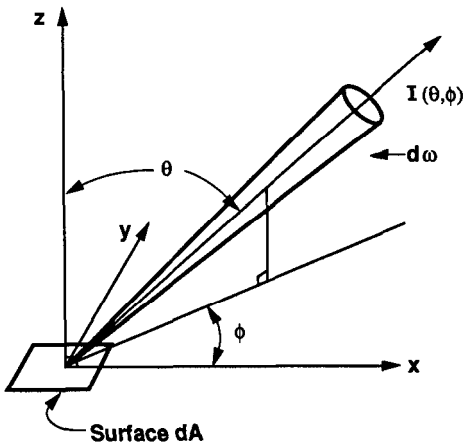

Fig. 1b. Geometry of light of intensity I leaving a surface element dA.

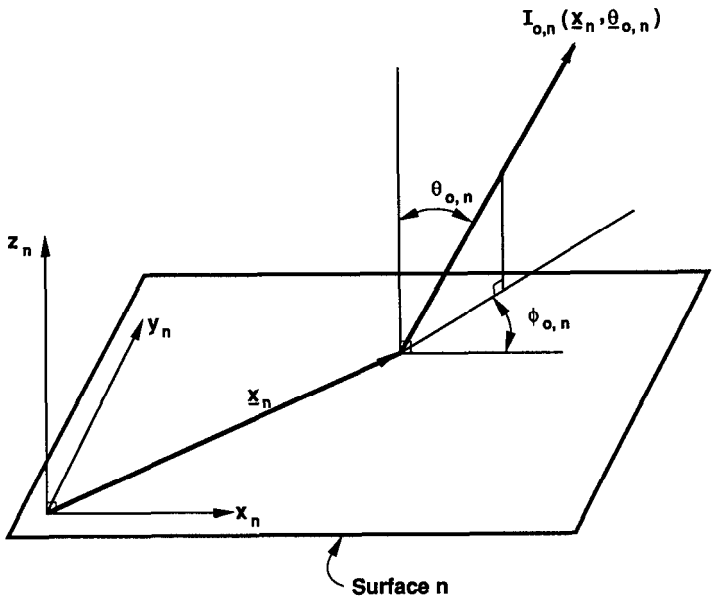

Fig. 1c. Definition of position vector $\underline{x}_n$ and direction vector $\underline{\theta}_{o,n}$.

transmitted light leaving surface n, expressed as

$$I_{o,n}(\underline{x}_n, \underline{\theta}_{o,n}) = I_{e,n}(\underline{x}_n, \underline{\theta}_{o,n}) + I_{r,n}(\underline{x}_n, \underline{\theta}_{o,n}) + I_{t,n}(\underline{x}_n, \underline{\theta}_{o,n}), \quad (2)$$

where the subscripts e, r, and t respectively denote the emitted, reflected, and transmitted components of the outgoing intensity.

In a typical scene, only a few surfaces, or light sources, emit light. For such emitters, the light source intensity $I_{e,n}(\underline{x}_n, \underline{\theta}_{o,n})$ in eq. (2) must be a given, independently prescribed function of position and direction. The second and third terms in eq. (2) are due to reflection and transmission, and couple the

intensity leaving surface n to the intensities arriving at n from all of the other surfaces in the environment. This introduces the reflectance and transmittance of the surface n, as described next.

Consider the geometry shown in Figure 2, in which an incident beam of energy flux density dq_i impinges with a solid angle $d\omega_i$ onto a surface. The subscript i denotes incident quantities. The direction of the incident beam is described by the angles (θ_i, ϕ_i) associated with a unit vector $\underline{\theta}_i$. In general, the incident beam will be reflected, absorbed, or transmitted at the surface. For discussion purposes the surface is assumed to be of a finite thickness, in which absorption occurs. The intensity of the reflected and transmitted components may display a complex directional pattern, as sketched by the intensity distributions $I_r(\underline{\theta}_r)$ and $I_t(\underline{\theta}_t)$ in Figure 2. The appropriate quantities to describe these distributions are the bidirectional reflectance and the bidirectional transmittance [2, 12], respectively defined by

$$\rho_{bd}(\underline{\theta}_r, \underline{\theta}_i) = \frac{dI_r(\underline{\theta}_r)}{dq_i(\underline{\theta}_i)}; \tag{3}$$

$$\tau_{bd}(\underline{\theta}_t, \underline{\theta}_i) = \frac{dI_t(\underline{\theta}_t)}{dq_i(\underline{\theta}_i)}. \tag{4}$$

Bidirectional refers to the two directions involved: the direction of illumination and the direction of either reflection or transmission. The bidirectional quantities are defined as ratios of the reflected or transmitted intensities to the incident energy.

Light that is not reflected or transmitted is absorbed. A parameter that describes the total amount of absorbed energy, as a function of incidence angle, is the absorptance,

$$\alpha(\underline{\theta}_i) = \frac{dq_{abs}}{dq_i(\underline{\theta}_i)}. \tag{5}$$

The light energy in the incident beam must be fully accounted for when light interacts with a surface. This leads to the following energy conservation statement at the surface, involving ρ_{db}, τ_{bd}, and α:

$$\int_{2\pi} \rho_{bd}(\underline{\theta}_i, \underline{\theta}_r) \cos\theta_r \, d\omega_r + \int_{2\pi} \tau_{bd}(\underline{\theta}_i, \underline{\theta}_t)\cos\theta_t \, d\omega_t + \alpha(\underline{\theta}_i) = 1. \tag{6}$$

The first integral is over the hemisphere of reflection angles above the surface, and the second is over the hemisphere of transmission angles below the surface. These integrals also serve to define, respectively, a reflectance for directional illumination and hemispherical reflection, ρ_{dh}, and a transmittance for directional illumination and hemispherical transmission, τ_{dh}. In terms of these quantities, eq. (6) becomes

$$\rho_{dh}(\underline{\theta}_i) + \tau_{dh}(\underline{\theta}_i) + \alpha(\underline{\theta}_i) = 1. \tag{7}$$

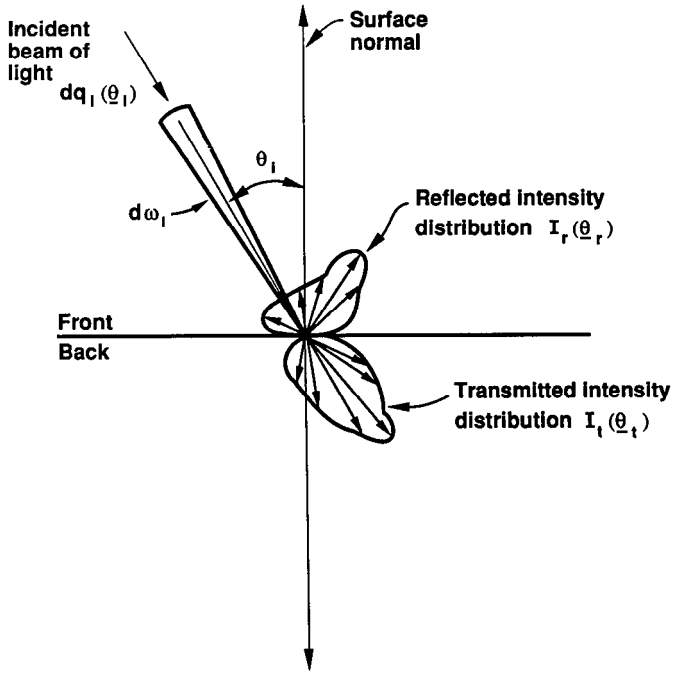

Fig. 2. General intensity distributions of reflected and transmitted light.

2.3 A General Equation for the Radiant Intensity of a Surface

The intensity leaving a surface n, $I_{o,n}$ is given by eq. (2). The second and third terms on the right side of this equation are developed in greater detail in this section. Specifically, using the definition of intensity in eq. (1) and integrating eq. (3) over the hemisphere of incident directions, the intensity of light $I_{r,n}$ reflected from surface n is

$$I_{r,n}(\underline{x}_n, \underline{\theta}_{o,n}) = \int_{2\pi} \rho_{bd,n}(\underline{\theta}_{if,n}, \underline{\theta}_{o,n}) I_{i,n}\underline{x}_n, \underline{\theta}_{if,n}) \cos\theta_{if,n}\, d\omega_{if,n}. \tag{8}$$

The subscript if,n denotes incident directions referred to the front of surface n.

Because intensity is constant along an unobstructed path, the intensity incident onto surface n, $I_{i,n}(\underline{x}_n, \underline{\theta}_{if,n})$, is equal to the intensity of radiation leaving another surface, say, m, which is visible from surface n. Let the latter intensity be denoted by $I_{o,m}(\underline{x}_m, \underline{\theta}_{o,m})$. The geometric relationship between surfaces n and m is sketched in Figure 3. A ray connecting points $\underline{x}_n$ and $\underline{x}_m$ on the two surfaces, as measured by coordinate systems fixed to the surfaces, makes angles of $\underline{\theta}_{if,n}$ and $\underline{\theta}_{o,m}$ with respect to the normals to the two surfaces as shown. Next, introduce a function $\mathbf{V}_r(\underline{x}_n, \underline{x}_m)$ that is unity if point $\underline{x}_m$ on the front of surface m is visible to point $\underline{x}_n$ when looking out from the front of surface n, and zero otherwise.

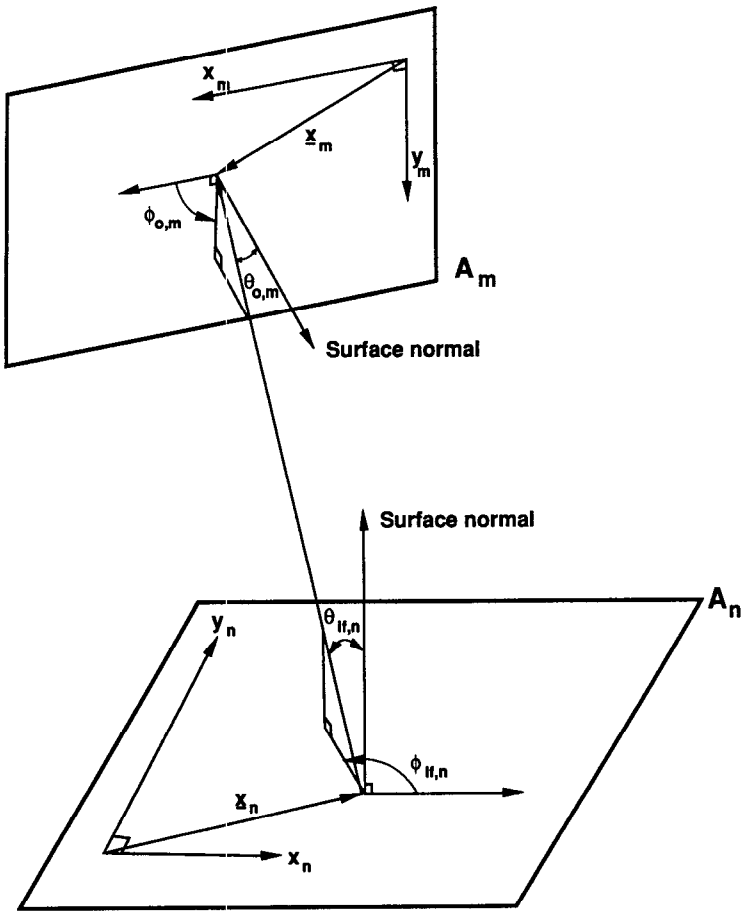

Fig. 3. Geometric relationship between surfaces n and m.

Thus, eq. (8) can be written as

$$I_{r,n}(\underline{x}_n, \underline{\theta}_{o,n}) = \sum_{m=1}^{N} \int_{A_m} \rho_{bd,n}(\underline{\theta}_{if,n}, \underline{\theta}_{o,n}) \mathbf{V}_r(\underline{x}_n, \underline{x}_m) I_{o,m}(\underline{x}_m, \underline{\theta}_{o,m}) \cos \theta_{if,n} \, d\omega_{if,n}, \tag{9}$$

where the summation is over the number of surfaces and the integration is over the area of each surface. Note that no generality has been lost in rewriting eq. (8) as eq. (9), since any environment can be considered a set of surfaces.

Similarly, an expression for transmitted intensity can be found by using eqs. (1) and (4). In the expression for transmitted intensity, the visibility function for reflection, $\mathbf{V}_r(\underline{x}_n, \underline{x}_m)$, is replaced by a visibility function for transmission, $\mathbf{V}_t(\underline{x}_n, \underline{x}_m)$, which is unity if a point $\underline{x}_m$ on the front of surface m is visible from a point $\underline{x}_n$ on the *back* of surface n, and zero otherwise. Introducing eq. (9) for $I_{r,n}$, and the analogous equation for $I_{t,n}$, into eq. (2), results in the

following general equation for $I_{o,n}$:

$$
\begin{aligned}
&I_{o,n}(\underline{x}_n, \underline{\theta}_{o,n}) \\
&\quad = I_{e,n}(\underline{x}_n, \underline{\theta}_{o,n}) \\
&\qquad + \sum_{m=1}^{N} \int_{A_m} \rho_{bd,n}(\underline{\theta}_{if,n}, \underline{\theta}_{o,n}) \mathbf{V}_r(\underline{x}_n, \underline{x}_m) I_{o,m}(\underline{x}_m, \underline{\theta}_{o,m}) \cos\theta_{if,n}\, d\omega_{if,n} \qquad (10) \\
&\qquad + \sum_{m=1}^{N} \int_{A_m} \tau_{bd,n}(\underline{\theta}_{ib,n}, \underline{\theta}_{o,n}) \mathbf{V}_t(\underline{x}_n, \underline{x}_m) I_{o,m}(\underline{x}_m, \underline{\theta}_{o,m}) \cos\theta_{ib,n}\, d\omega_{ib,n}.
\end{aligned}
$$

The subscript ib,n denotes incident directions on the back of surface n.

An equation of the form of eq. (10) holds for each of the N surfaces in the environment. The solution of the system of N simultaneous integral equations yields the N intensity functions $I_{o,n}(\underline{x}_n, \underline{\theta}_{o,n})$.

3. SIMPLIFICATIONS FOR IDEAL SURFACE REFLECTION/TRANSMISSION

The general equation for the radiant intensity of a surface, eq. (10), is the appropriate starting point for deriving a lighting model. However, eq. (10) is difficult to use directly, because it allows complicated directional and spatial dependencies of the bidirectional quantities (ρ_{bd}, τ_{bd}) and the intensities (I_o, I_e). It is helpful to express the directional dependencies of I_e, ρ_{bd}, and τ_{bd} in terms of simplified, yet still fairly general, models. Models that have produced useful results in radiative heat transfer include ideal diffuse, ideal specular, and combined diffuse/specular behavior. Use of the simplified models results in a revised equation of transport, eq. (15).

Light is said to be ideal diffuse when the light intensity is independent of direction. The case of ideal diffuse emission is sketched in Figure 4a. For ideal diffuse emission, the light source term in eq. (10) becomes simply $I_{e,n}(\underline{x}_n)$, a position-dependent light intensity.

Ideal diffuse reflection and transmission are sketched in Figure 4b. For this case the intensities $I_{r,n}$ and $I_{t,n}$ are independent of direction. When ideal diffuse behavior is assumed, $\rho_{bd}(\underline{\theta}_i, \underline{\theta}_r)$ and $\tau_{bd}(\underline{\theta}_i, \underline{\theta}_t)$ in eq. (10) may be replaced by ρ_d/π and τ_d/π, where the subscripts denote *diffuse*. (For an ideal diffuse surface, ρ_d and τ_d are the directional-hemispherical reflectance and transmittance, respectively, as defined by eqs. (6) and (7)). From thermodynamics it can be shown that the diffuse assumption implies that ρ_d and τ_d must be independent of $\underline{\theta}_i$.

If the emission, reflection, and transmission are all ideal diffuse, it is impossible to distinguish between them in the emergent radiation from a surface. Also, the outgoing intensity $I_{o,n}$ does not vary with angle, and the intensity definition, eq. (1), may be integrated to obtain

$$\pi I_{o,n}(\underline{x}_n) = q_{o,n}(\underline{x}_n) \equiv B_n(\underline{x}_n). \qquad (11)$$

This provides a useful relationship between $I_{o,n}$ and the radiosity, B_n, for the special case of a fully diffuse surface.

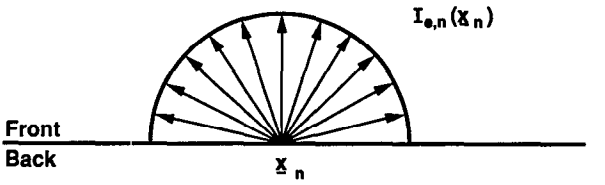

Fig. 4a. Intensity distribution of ideal diffuse emission.

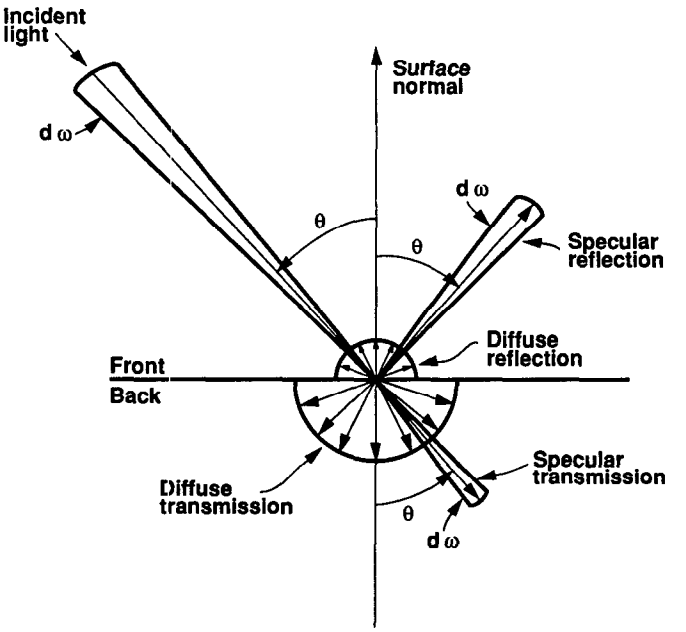

Fig. 4b. Intensity distribution of ideal diffuse and ideal specular reflection and transmission.

Directional distributions for ideal specular reflection and ideal specular transmission are also shown in Figure 4b. In this case, the bidirectional reflectance is zero except when (θ_r, ϕ_r) is equal to $(\theta_i, \phi_i + \pi)$, and the bidirectional transmittance is zero except when (θ_t, ϕ_t) is equal to $(\pi - \theta_i, \phi_i + \pi)$. Note that the latter neglects refraction effects at the interface. At a refracting surface, the bidirectional transmittance is zero except when (θ_t, ϕ_t) is equal to $(\pi - \theta_i^*, \phi_i + \pi)$, where θ_i^* is related to θ_i by Snell's law. Such effects can be included, but, in the interests of simplicity, are neglected in this paper. The neglect of refraction is valid if the interface is a thin transmitting plate, such as a window. In what follows, a nonrefracting surface will be referred to as a specular transmitter. Ideal specular behavior is usually expressed in terms of a reflectance and a

transmittance defined as ratios of intensities:

$$\rho_s = \frac{I_r}{I_i}, \tag{12}$$

$$\tau_s = \frac{I_t}{I_i}. \tag{13}$$

It is understood that I_r and I_t are zero except in the specular reflection or transmission directions, respectively.

The ideal diffuse and ideal specular behaviors shown in Figure 4b represent approximations to the behavior of real materials. A somewhat more general approximation is possible by superposing the two limits. When ρ_{bd} and τ_{bd} are written as linear combinations of ideal diffuse and ideal specular behavior, conservation of energy, as expressed in eq. (6), requires that

$$\rho_s + \rho_d + \tau_s + \tau_d + \alpha = 1. \tag{14}$$

When the reflection/transmission coefficients are taken as constant over each area A_n, the general equation for the radiant intensity of a surface, eq. (10), becomes

$$\begin{aligned} I_{o,n}(\underline{x}_n, \underline{\theta}_{o,n}) = {} & I_{e,n}(\underline{x}_n, \underline{\theta}_{o,n}) \\ & + \frac{\rho_{d,n}}{\pi}\left\{\sum_{m=1}^{N}\int_{A_m} \mathbf{V}_r(\underline{x}_n, \underline{x}_m) I_{o,m}(\underline{x}_m, \underline{\theta}_{o,m})\cos\theta_{if,n}\, d\omega_{if,n}\right\} \\ & + \rho_{s,n} I_{o,n(s)}(\underline{x}_{n(s)}, \underline{\theta}_{n(s)}) \\ & + \frac{\tau_{d,n}}{\pi}\left\{\sum_{m=1}^{N}\int_{A_m} \mathbf{V}_t(\underline{x}_n, \underline{x}_m) I_{o,m}(\underline{x}_m, \underline{\theta}_{o,m})\cos\theta_{ib,n}\, d\omega_{ib,n}\right\} \\ & + \tau_{s,n} I_{o,n(t)}(\underline{x}_{n(t)}, \underline{\theta}_{n(t)}). \end{aligned} \tag{15}$$

Note that the ideal diffuse assumption is not invoked for $I_{e,n}$ in eq. (15). As shown in Figure 5, $n(s)$ denotes the surface intersected by a ray leaving point $\underline{x}_n$ in the specular reflection direction $(\theta_{o,n}, \phi_{o,n} + \pi)$, and $n(t)$ denotes the surface intersected by a ray leaving $\underline{x}_n$ in the specular transmission direction $(\pi - \theta_{o,n}, \phi_{o,n} + \pi)$. Appropriate forms of eq. (15) for purely diffuse or purely specular environments are found by setting $\rho_{s,n} = \tau_{s,n} = 0$, or $\rho_{d,n} = \tau_{d,n} = 0$, respectively.

4. DERIVATION OF RADIOSITY AND RAY-TRACING METHODS

The basic radiosity method and a basic form of ray tracing are derived from eq. (15) in this section. The assumptions are contrasted, and the failure of ad hoc combinations of the two approaches is discussed.

4.1 The Radiosity Method

In the basic radiosity method, all emission and reflection processes are assumed to be ideal diffuse, and all surfaces are taken as opaque. Thus, in

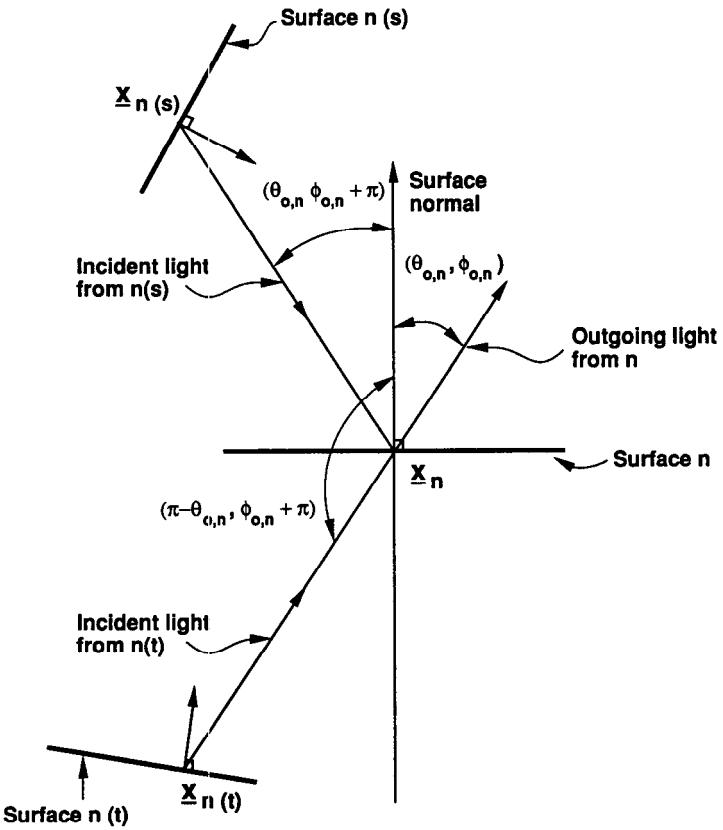

Fig. 5. Surfaces n(s) and n(t) from which light is specularly reflected and transmitted, respectively, by surface n into the direction of interest $\underline{\theta}_{o,n}$.

eq. (15), $\rho_s = \tau_s = \tau_d = 0$. Since $I_{o,n}$ is independent of direction, eq. (15) reduces to

$$I_{o,n}(\underline{x}_n) = I_{e,n}(\underline{x}_n) + \frac{\rho_{d,n}}{\pi} \sum_{m=1}^{N} \int_{Am} \mathbf{V}_r(\underline{x}_n, \underline{x}_m) I_{o,m}(\underline{x}_m) \cos\theta_{if,n}\, d\omega_{if,n}. \quad (16)$$

Further, the assumption is made that $I_{o,n}$ and $I_{e,n}$ are constant for each surface n. After averaging eq. (16) over the area A_n, there results

$$I_{o,n} = I_{e,n} + \frac{\rho_{d,n}}{\pi} \sum_{m=1}^{N} \left(\frac{I_{o,m}}{A_n}\right) \int_{A_n} \int_{A_m} \mathbf{V}_r(\underline{x}_n, \underline{x}_m) \cos\theta_{if,n}\, d\omega_{if,n}\, dA_n$$

or (17)

$$I_{o,n} = I_{e,n} + \rho_{d,n} \sum_{m=1}^{N} I_{o,m} F_{nm}.$$

The second equation serves to define the forward diffuse form factor F_{nm}, which depends on geometry alone. F_{nm} denotes the fraction of diffuse energy leaving surface n that impinges on surface m.

Equation (17) is the basic radiosity method. Since eq. (11) applies, the intensities may be replaced by radiosities by using $I_{o,n} = B_n/\pi$.

4.2 A Basic Ray-Tracing Method

A brief outline of a basic ray-tracing method [14] will now be given. The necessary assumptions were originally outlined by Cook, Porter, and Carpenter [2]. The term *basic* is used because many sophisticated ray-tracing variations have been developed that will not be considered here.

In a basic ray-tracing method, light sources are assumed to be small and to be nonreflectors and nontransmitters of other light. The governing equations either have only the first term on the right side of eq. (15), or only the other four terms. Since the light source intensities are given, only the second category of equations needs to be considered. Diffuse transmission is also usually neglected, so that $\tau_d = 0$. The ray-tracing equation, derived from eq. (15), becomes

$$\begin{aligned} I_{o,n}(\underline{x}_n, \underline{\theta}_{o,n}) = {} & \frac{\rho_{d,n}}{\pi} \sum_{l=1}^{L} \mathbf{V}_r(\underline{x}_n, \underline{x}_l) I_{e,l} \cos\theta_{if,n} \Delta\omega_{if,n} \\ & + \frac{\rho_{d,n}}{\pi} \sum_{m=L+1}^{N} \int_{A_m} \mathbf{V}_r(\underline{x}_n, \underline{x}_m) I_{o,m}(\underline{x}_m, \underline{\theta}_{o,m}) \cos\theta_{if,n} \, d\omega_{if,n} \\ & + \rho_{s,n} I_{o,n(s)}(\underline{x}_{n(s)}, \underline{\theta}_{o,n(s)}) + \tau_{s,n} I_{o,n(t)}(\underline{x}_{n(t)}, \underline{\theta}_{o,n(t)}). \end{aligned} \tag{18}$$

The surfaces that are light sources, L in number, have been placed in the first summation.

Next, assume all light intensities $I_{o,m}$ not multiplied by ρ_s or τ_s in eq. (18) can be lumped into an average intensity I_a, usually called the *ambient intensity*. Further, by taking I_a outside of the integral and defining the coefficient that remains to be ρ_a, a term $\rho_a I_a$ appears. Thus, the governing equation for the intensity leaving a point becomes

$$\begin{aligned} I_{o,n}(\underline{x}_n, \underline{\theta}_{o,n}) = {} & \frac{\rho_{d,n}}{\pi} \sum_{l=1}^{L} \mathbf{V}_r(\underline{x}_n, \underline{x}_l) I_{e,l} \cos\theta_{if,n} \Delta\omega_{if,n} + \rho_a I_a \\ & + \rho_{s,n} I_{o,n(s)}(\underline{x}_{n(s)}, \underline{\theta}_{o,n(s)}) + \tau_{s,n} I_{o,n(t)}(\underline{x}_{n(t)}, \underline{\theta}_{o,n(t)}). \end{aligned} \tag{19}$$

To obtain an explicit equation for $I_{o,n}$, the terms I_a, $I_{o,n(s)}$, and $I_{o,n(t)}$ must be expressed in terms of light source intensities. In principle, I_a should account for the light intensity of every surface visible from $\underline{x}_n$. In practice, I_a is usually assigned a constant value for all surfaces.

The points $\underline{x}_{n(s)}$ and $\underline{x}_{n(t)}$ are found by the intersections of rays with surfaces. The intensities at these intersection points, $I_{o,n(s)}$ and $I_{o,n(t)}$, are also governed by eq. (19). Further rays must be cast to determine the appropriate next intersections. Thus, eq. (19), when expressed in terms of light source intensities, has an infinite number of terms, implying the need for a tree of ray intersections of infinite depth. As the depth increases, the contribution of each additional term diminishes. Thus, in practice, the depth of the tree can be limited.

4.3 Simple Superposition

In the radiosity method, only the energy exchange between diffusely reflecting surfaces is calculated, assuming that any other energy exchange is insignificant. In the ray-tracing method, only the energy exchange between surfaces with strongly directional properties is assumed to be important. In the simplest superposition of the two approaches, the first two terms of eq. (19) would be replaced by intensities calculated with the radiosity method. However, this superposition omits energy that is received by diffusely reflecting surfaces from surfaces with strongly directional properties. To account for this energy, an alternative approach, starting with eq. (15), is needed.

5. THE EXTENDED RADIOSITY METHOD

In this section an extended radiosity method is derived from the surface intensity equation, eq. (15). This equation assumes that all surfaces are ideal specular, ideal diffuse, or ideal linear combinations of the two. The extended method places no additional restrictions on diffuse/specular behavior, and includes reflection and transmission processes. In what follows, the basic radiosity method is extended in steps, by adding diffuse transmission, specular transmission, and, finally, specular reflection. The last step results in the extended method given in Section 5.3.

5.1 Diffuse Transmission

In the extension of the radiosity method to include diffuse transmission [4, 12], surfaces are modeled as ideal diffuse reflectors and transmitters. Emission is assumed to be ideal diffuse. Neglecting specular behavior ($\rho_s = \tau_s = 0$) and assuming $I_{o,n}$ and $I_{e,n}$ are constant for each surface, the surface intensity relation, eq. (15), simplifies to

$$I_{o,n} = I_{e,n} + \rho_{d,n} \sum_{m=1}^{N} I_{o,m} F_{nm} + \frac{\tau_{d,n}}{\pi} \sum_{m=1}^{N} \frac{I_{o,m}}{A_n} \int_{A_n} \int_{A_m} \mathbf{V}_t(\underline{x}_n, \underline{x}_m) \cos \theta_{ib,n} \, d\omega_{ib,n} \, dA_n \tag{20a}$$

or

$$I_{o,n} = I_{e,n} + \rho_{d,n} \sum_{m=1}^{N} I_{o,m} F_{nm} + \tau_{d,n} \sum_{m=1}^{N} I_{o,m} T_{nm}. \tag{20b}$$

The forward diffuse form factor F_{nm} now denotes the fraction of diffuse energy leaving n from its *front* side and impinging on m. A new form factor, T_{nm}, arises through the transmission term. This is the backward diffuse form factor, which denotes the fraction of diffuse energy leaving n from its *back* side and impinging on surface m. The two form factors are similar mathematically, except that the integration with respect to surface n is over the front hemisphere of solid angles for F_{nm} and over the back hemisphere for T_{nm}.

5.2 Specular Transmission

The extension to include specular transmission introduces additional geometrical complexity [12]. Now neglecting specular reflection ($\rho_s = 0$), but including $\rho_{d,n}$, $\tau_{d,n}$, and $\tau_{s,n}$, and assuming ideal diffuse emission, eq. (15) reduces to

$$\begin{aligned} I_{o,n}(\underline{x}_n, \underline{\theta}_{o,n}) &= I_{e,n}(\underline{x}_n) + \frac{\rho_{d,n}}{\pi} \sum_{m=1}^{N} \int_{A_m} \mathbf{V}_r(\underline{x}_n, \underline{x}_m) I_{o,m}(\underline{x}_m, \underline{\theta}_{o,m}) \cos\theta_{if,n}\, d\omega_{if,n} \\ &\quad + \frac{\tau_{d,n}}{\pi} \sum_{m=1}^{N} \int_{A_m} \mathbf{V}_t(\underline{x}_n, \underline{x}_m) I_{o,m}(\underline{x}_m, \underline{\theta}_{o,m}) \cos\theta_{ib,n}\, d\omega_{ib,n} \\ &\quad + \tau_{s,n} I_{o,n(t)}(\underline{x}_{n(t)}, \underline{\theta}_{n(t)}). \end{aligned} \tag{21}$$

Note that the intensity $I_{o,n}$ depends on $(\underline{x}_n, \underline{\theta}_{o,n})$ due to the ideal specular component of the transmittance. Let $I_{o,n}$ be separated into two components—an ideal diffuse component $I_{od,n}$ and an ideal specular component $I_{os,n}$—defined by

$$\begin{aligned} I_{od,n}(\underline{x}_n) = I_{e,n}(\underline{x}_n) &+ \frac{\rho_{d,n}}{\pi} \sum_{m=1}^{N} \int_{A_m} \mathbf{V}_r(\underline{x}_n, \underline{x}_m) I_{o,m}(\underline{x}_m, \underline{\theta}_{o,m}) \cos\theta_{if,n}\, d\omega_{if,n} \\ &+ \frac{\tau_{d,n}}{\pi} \sum_{m=1}^{N} \int_{A_m} \mathbf{V}_t(x_n, x_m) I_{o,m}(\underline{x}_m, \underline{\theta}_{o,m}) \cos\theta_{ib,n}\, d\omega_{ib,n} \end{aligned} \tag{22a}$$

and

$$I_{os,n}(\underline{x}_n, \underline{\theta}_{o,n}) = \tau_{s,n} I_{o,n(t)}(\underline{x}_{n(t)}, \underline{\theta}_{o,n(t)}). \tag{22b}$$

With this definition, $I_{os,n}$ depends on direction, but $I_{od,n}$ does not.

The intensity $I_{o,m}$ on the right of eq. (22a) can similarly be expressed as the sum of $I_{od,m}$ and $I_{os,m}$. Assume that no two ideal specular surfaces are visible to one another. The specular component of intensity for a surface m can then be expressed as

$$I_{os,m}(\underline{x}_m, \underline{\theta}_{o,m}) = \tau_{s,m} I_{od,m(t)}(\underline{x}_{m(t)}). \tag{23}$$

The equation for $I_{od,n}$ can now be written in terms of diffuse intensities:

$$\begin{aligned} I_{od,n}(\underline{x}_n) &= I_{e,n}(\underline{x}_n) \\ &\quad + \frac{\rho_{d,n}}{\pi} \sum_{m=1}^{N} \int_{A_m} \mathbf{V}_r(\underline{x}_n, \underline{x}_m) \{I_{od,m}(\underline{x}_m) + \tau_{s,m} I_{od,m(t)}(\underline{x}_{m(t)})\} \cos\theta_{if,n}\, d\omega_{if,n} \\ &\quad + \frac{\tau_{d,n}}{\pi} \sum_{m=1}^{N} \int_{A_m} \mathbf{V}_t(\underline{x}_n, \underline{x}_m) \{I_{od,m}(\underline{x}_m) + \tau_{s,m} I_{od,m(t)}(\underline{x}_{m(t)})\} \cos\theta_{ib,n}\, d\omega_{ib,n}. \end{aligned} \tag{24}$$

Note the absence of a directional dependence for the Is on the right side, and that only one additional term arises inside the braces to account for specular transmission.

As before, assume that the diffuse component of intensity is constant over each surface. The integrals involving diffuse intensity $I_{\mathrm{od},m}$ in the second and third terms on the right of eq. (24) can be replaced by $I_{\mathrm{od},m}F_{nm}$ and $I_{\mathrm{od},m}T_{nm}$, respectively, where F_{nm} and T_{nm} are forward and backward form factors.

The integral of intensity $I_{\mathrm{o},m(\mathrm{t})}$ in eq. (24) is diagramed in Figure 6. $I_{\mathrm{o},m(\mathrm{t})}$ is the intensity of the surface $m(\mathrm{t})$ that is visible through surface m (in this case surface p). The integral over A_m can be written as the sum of the integrals over the surfaces A_p that are visible through specularly transmitting surfaces m. That is,

$$\sum_{m=1}^{N} \tau_{\mathrm{s},m} \int_{A_m} \mathbf{V}_{\mathrm{r}}(\underline{x}_n, \underline{x}_m) I_{\mathrm{o},m(\mathrm{t})} \cos\theta_{\mathrm{if},n}\, d\omega_{\mathrm{if},n} = \sum_{m=1}^{N} \tau_{\mathrm{s},m} \sum_{p=1}^{N} I_{\mathrm{od},p} \int_{A_p} \mathbf{V}_{\mathrm{r}}(\underline{x}_n, \underline{x}_m, \underline{x}_p) \cos\theta_{\mathrm{if},n}\, d\omega_{\mathrm{if},n}. \tag{25}$$

The function $\mathbf{V}_{\mathrm{r}}$ with three parameters indicates that point $\underline{x}_n$, when viewing a point $\underline{x}_m$ on m, can see point $\underline{x}_p$ on p. The integral over A_p in eq. (25) represents a geometric factor that will be denoted by $T_{\mathrm{f},nmp}$. This factor is equal to the form factor F_{np}, if calculated using surface m as a restrictive window in the environment. Thus, eq. (24) becomes

$$I_{\mathrm{od},n} = I_{e,n} + \rho_{\mathrm{d},n} \sum_{m=1}^{N} \left\{ I_{\mathrm{od},m}F_{nm} + \tau_{\mathrm{s},m} \sum_{p=1}^{N} I_{\mathrm{od},p}T_{\mathrm{f},nmp} \right\} + \tau_{\mathrm{d},n} \sum_{m=1}^{N} \left\{ I_{\mathrm{od},m}T_{nm} + \tau_{\mathrm{s},m} \sum_{p=1}^{N} I_{\mathrm{od},p}T_{\mathrm{b},nmp} \right\}. \tag{26}$$

$T_{\mathrm{b},nmp}$ is given by the same integral as $T_{\mathrm{f},nmp}$, except that the integration is over the hemisphere of directions on the back of surface n.

5.3 General Case

The addition of specular reflection leads to the most general case. Both reflection and transmission are written as linear combinations of ideal specular and ideal diffuse behavior. This case represents a straightforward extension of the results of the previous section [5].

The starting point is again eq. (15). Ideal diffuse emission is assumed, and $\rho_{\mathrm{d},n}$, $\rho_{\mathrm{s},n}$, $\tau_{\mathrm{d},n}$, and $\tau_{\mathrm{s},n}$ are included for all surfaces. Diffuse and specular components of intensity are defined. The equation for the diffuse intensity is the same as eq. (22). The equation for the specular intensity is

$$I_{\mathrm{os},m}(\underline{x}_m, \underline{\theta}_{\mathrm{o},m}) = \tau_{\mathrm{s},m} I_{\mathrm{o},m(\mathrm{t})}(\underline{x}_{m(\mathrm{t})}, \underline{\theta}_{m(\mathrm{t})}) + \rho_{\mathrm{s},m} I_{\mathrm{o},m(\mathrm{s})}(\underline{x}_{m(\mathrm{s})}, \underline{\theta}_{m(\mathrm{s})}). \tag{27}$$

The approach in [5] allows any number of specular surfaces. In this paper only specular reflecting surfaces that are not visible to one another, or to specularly transmitting surfaces, are considered. The specular component of intensity can then be written as

$$I_{\mathrm{os},m}(\underline{x}_m, \underline{\theta}_{\mathrm{o},m}) = \tau_{\mathrm{s},m} I_{\mathrm{od},m(\mathrm{t})}(\underline{x}_{m(\mathrm{t})}) + \rho_{\mathrm{s},m} I_{\mathrm{od},m(\mathrm{s})}(\underline{x}_{m(\mathrm{s})}). \tag{28}$$

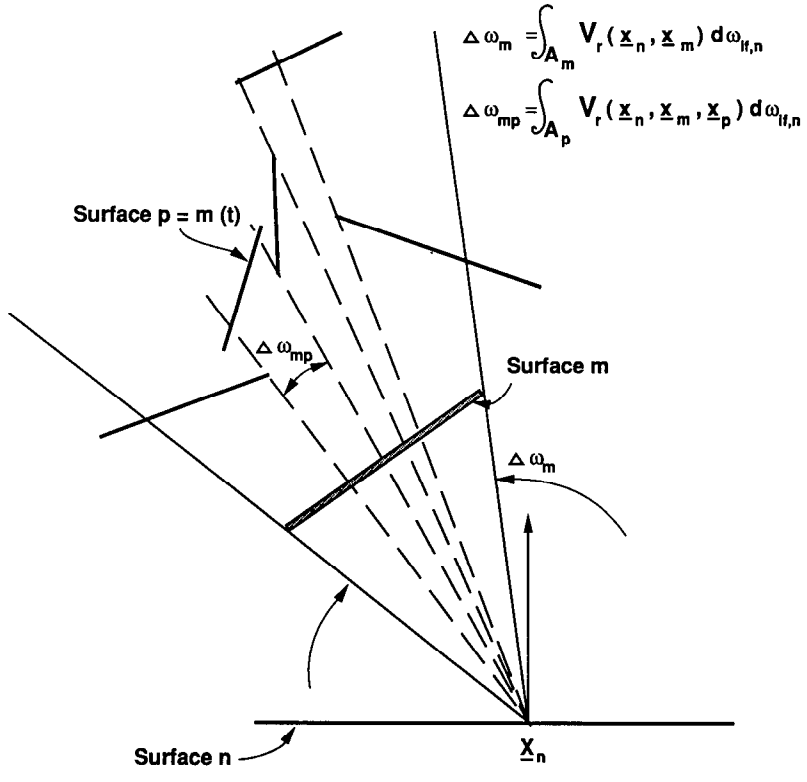

Fig. 6. The integral of light intensity over a specularly transmitting surface m is equal to the sum of the integrals of light intensity over the surfaces p that are visible through surface m.

Consider Figure 7, in which a surface m serves to create a mirror image p', as seen from n, of the surface p. Thus, the problem of specular reflection from the real environment can be replaced by the problem of specular transmission from a virtual environment.

Once again, assume the diffuse component of intensity is constant over each surface. Equation (22) for $I_{od,n}$ becomes

$$I_{od,n} = I_{e,n} + \rho_{d,n} \sum_{m=1}^{N} \left\{ I_{od,m} F_{nm} + \tau_{s,m} \sum_{p=1}^{N} I_{od,p} T_{f,nmp} + \rho_{s,m} \int_{A_m} V_r(\underline{x}_n, \underline{x}_m) I_{od,m'(t)} \cos\theta_{if,n}\, d\omega_{if,n} \right\}$$
$$+ \tau_{d,n} \sum_{m=1}^{N} \left\{ I_{od,m} T_{nm} + \tau_{s,m} \sum_{p=1}^{N} I_{od,p} T_{b,nmp} + \rho_{s,m} \int_{A_m} V_t(\underline{x}_n, \underline{x}_m) I_{od,m'(t)} \cos\theta_{ib,n}\, d\omega_{ib,n} \right\}. \quad (29)$$

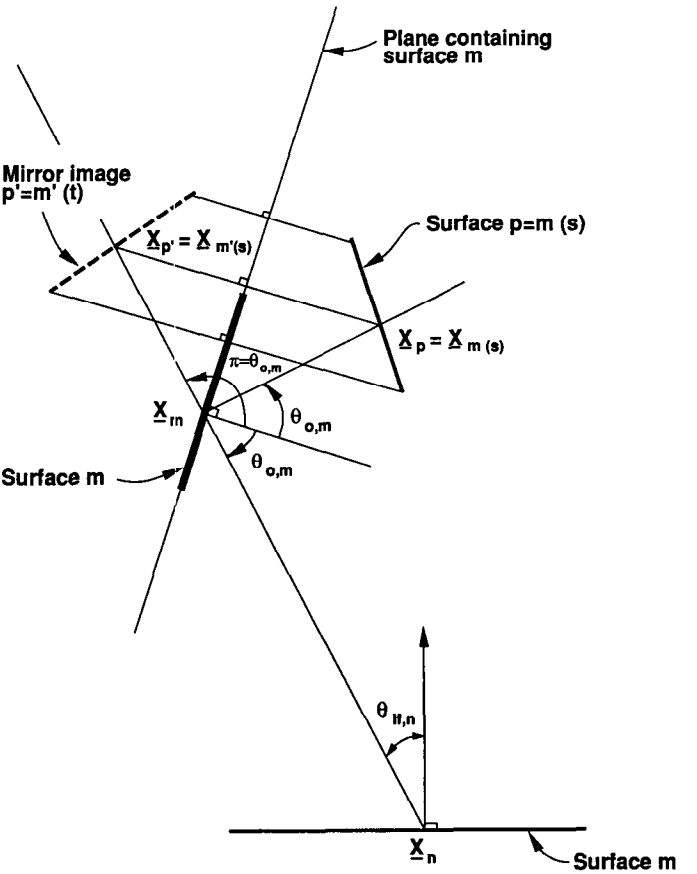

Fig. 7. From point $\underline{x}_n$, a mirror image p' of the real surface p can be seen in the specularly reflecting surface m. Finding the point $\underline{x}_p$ from which light is specularly reflected from surface m to surface n is equivalent to finding the point $\underline{x}_{p'}$ from which light is specularly transmitted through surface m.

The integrals over A_m in eq. (29) can be written as the sum over all virtual surfaces p' that are visible through surface m, or

$$\sum_{m=1}^{N} \rho_{s,m} \int_{A_m} \mathbf{V}_r(\underline{x}_n, \underline{x}_m) I_{od,m'(t)} \cos \theta_{if,n} \, d\omega_{if,n} = \sum_{m=1}^{N} \rho_{s,m} \sum_{p=1}^{N} I_{od,p} \int_{A_{p'}} \mathbf{V}_r(\underline{x}_n, \underline{x}_m, \underline{x}_{p'}) \cos \theta_{if,n} \, d\omega_{if,n}. \tag{30}$$

The integral over $A_{p'}$ is a geometric factor, which will be denoted by $F_{f,nmp}$, and will be referred to as the forward mirror form factor. $F_{f,nmp}$ is equal to the factor $F_{np'}$ if the virtual environment is viewed through a window formed by surface m. Similarly, the integral over the hemisphere behind surface n can be written as a

factor $F_{b,nmp}$, the backward mirror form factor. Using these factors, eq. (29) for $I_{od,n}$ is

$$I_{od,n} = I_{e,n} + \rho_{d,n} \sum_{m=1}^{N} \left\{ I_{od,m} F_{nm} + \tau_{s,m} \sum_{p=1}^{N} I_{od,p} T_{f,nmp} + \rho_{s,m} \sum_{p=1}^{N} I_{od,p} F_{f,nmp} \right\} + \tau_{d,n} \sum_{m=1}^{N} \left\{ I_{od,m} T_{nm} + \tau_{s,m} \sum_{p=1}^{N} I_{od,p} T_{b,nmp} + \rho_{s,m} \sum_{p=1}^{N} I_{od,p} F_{b,nmp} \right\}. \tag{31}$$

Because no two specular surfaces are visible to one another or to any specularly transmitting surface, the diffuse and specular components of intensity in eqs. (31) and (28) are decoupled. The diffuse component of intensity for all surfaces is found by solving the set of simultaneous equations given in eq. (31). While eq. (31) includes more terms, the number of equations is the same as if all surfaces were diffuse. This solution is view independent. Once a view direction has been selected, the specular components are found from eq. (28) by ray tracing with a tree depth of one. The result is a two-pass solution procedure, as described in [13].

The extended method is readily generalized to any number of specular surfaces in arbitrary arrangement [11]. When two or more specular surfaces see one another, additional factors must be introduced into eq. (31), leading to added complexity [5]. These factors allow a higher number of specular interreflections/transmissions. Conservation of energy, as expressed in eq. (14), dictates that with each interreflection/transmission the light intensity is attenuated. Consequently, in most environments, the first specular reflection/transmission is the most important for the illumination of diffuse surfaces. Thus, the present extended method, which does not allow multiple interreflections/transmissions, is rigorously valid when specular surfaces do not see one another, but is generally a good approximation even in cases when they do. In fact, cases for which the multiple reflections from specular surfaces will have a visible impact on the illumination of a diffuse surface must be carefully constructed. An example would be laser light in a darkroom reflecting through a series of mirrors making a spot on a diffuse piece of paper.

6. FORM FACTOR ALGORITHMS

The form factors appearing in eq. (31) are evaluated using extensions of the hemicube algorithm [1].

6.1 Hemicube Algorithm

The forward diffuse form factor is given by

$$F_{nm} = \frac{1}{\pi A_n} \int_{A_n} \int_{A_m} \mathbf{V}_r(\underline{x}_n, \underline{x}_m) \cos \theta_{if,n} \, d\omega_{if,n} \, dA_n. \tag{32}$$

If surfaces in the environment are divided into sufficiently small areas, the integral over A_n can be approximated by the value of the inner integral at the center of A_n:

$$F_{nm} \simeq \frac{1}{\pi} \int_{A_m} \mathbf{V}_r(\underline{x}_n, \underline{x}_m) \cos \theta_{if,n} \, d\omega_{if,n}. \tag{33}$$

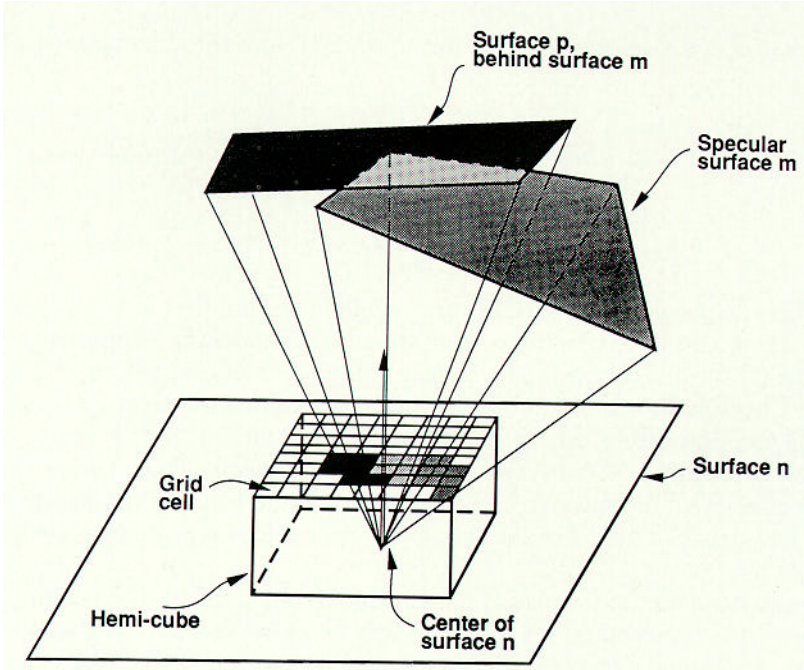

Fig. 8. Finding form factors using a hemicube constructed over the center of surface n. For clarity, grid cells are shown only on the top face of the hemicube. The window form factor, $T_{f,nmp}$, is equal to the sum of factors associated with the grid cells through which surface p is visible through surface m.

A fictitious hemicube is placed over the center of the surface A, for which form factors are to be found, as shown in Figure 8. Each side of the hemicube is divided into grid cells. A form factor can be determined analytically for each grid cell. The grid cells through which surface m is visible to surface n are found efficiently by using the depth buffer algorithm. The form factor F_{nm} is equal to the sum of the form factors associated with the grid cells through which surface m is visible to surface n.

6.2 Backward Diffuse Form Factors

The form factors T_{nm} are calculated in the same manner as the factors F_{nm}, except that the hemicube is placed on the back of the surface A_i. Frequently a diffusely transmitting object will be defined as two surfaces, say, i and j, defined by the same coordinates, but that have opposite designations of front and back. In this case additional calculations are not needed to find T_{jm} and T_{im}, since $T_{jm} = F_{im}$ and $T_{im} = F_{jm}$.

6.3 Window Form Factors

A specularly transmitting surface is treated as a window restricting the view of the environment, as shown in Figure 8. For each surface n, surfaces in front of the transmitting surface are checked to see if they obscure the transmitting surface. Surfaces behind the transmitting surface are checked to see if they are visible through the transmitting surface. The factor $T_{f,nmp}$ is equal to the sum of

the form factors associated with the grid cells through which surface p is visible to surface n through surface m. The backward form factors $T_{b,nmp}$ are similarly constructed, except the hemicube is positioned on the back of surface n.

6.4 Mirror Image Form Factors

A specularly reflecting surface is treated as a window in the real environment, through which the mirror image of the real environment is seen. Coordinates are calculated to define the virtual images of all real surfaces. For each surface n, the real surfaces in front of the mirror surface are checked to see if they obscure the view that n has of the mirror surface. Virtual surfaces behind the mirror surface are checked to see if they are visible through the mirror surface. Graphically, the process of finding mirror image form factors $F_{f,nmp}$ is the same as in Figure 8, except that the surface behind the mirror surface is a virtual surface. The factors $F_{b,nmp}$ are found either by constructing a hemicube on the back side of the surface or by defining transmitting surfaces in pairs.

The algorithms for the window and mirror form factors discussed above can be applied when the specular surfaces (either reflectors or transmitters) are planar and the transmitting surfaces are very thin. As mentioned in [13], window and mirror form factors for specular surfaces of arbitrary geometry can be calculated by finding the real or virtual surfaces behind the specular surface by ray tracing, rather than by using the depth buffer algorithm.

7. IMPLEMENTATION OF THE EXTENDED METHOD

The implementation of the extended method begins by defining the geometry and optical properties (i.e., I_e, ρ, and τ) of each surface. These definitions are used to find the forward diffuse form factors, and the backward, window, and mirror form factors, if necessary. The form factors are used to form a set of simultaneous algebraic equations, of the form of eq. (31), for the diffuse intensities of all surfaces. The image is rendered by summing the diffuse intensity calculated by bilinear interpolation across each surface, and the specular intensity calculated by ray tracing.

As in the basic radiosity method, if the geometry is unchanged, new form factors are not needed to solve for intensities when I_e, ρ, and τ are changed. If a different view of an environment is needed, only the rendering step needs to be redone.

Images illustrating results from the extended method are shown in Figures 9–11. These figures demonstrate extensions of the basic radiosity method. Approximate times to generate the form factors required for each environment ranged from 30 to 60 cpu minutes on a VAX 8700. Approximate times for solving the simultaneous equations for each lighting condition ranged from 5 to 8 cpu minutes. Rendering each image at a resolution of 1000 × 1000 pixels required 5 to 10 cpu minutes.

Figure 9 shows a pole lamp with a diffusely transmitting shade in an otherwise empty room. The room walls are opaque and diffuse. The bulb in the lamp is modeled as a cube with emitting white sides. The shade is modeled as eight red transmitting surfaces. The diffuse transmission through the shade is clearly

Fig. 9. Light transmitted diffusely through a lamp shade. Light that reaches the ceiling, walls, and floors directly from the light bulb is white; light that is diffusely transmitted through the shade is red.

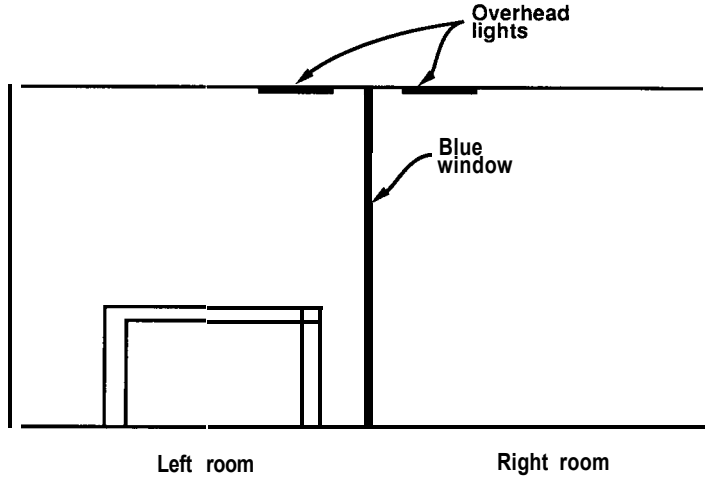

Fig. 10a. Diagram of two rooms that share a wall containing a blue, specularly transmitting, window.

visible. The light on the walls shows the contrast between diffusely transmitted light and light received directly from the bulb. No superposition of radiosity and ray tracing could account for the diffusely transmitted light and its diffuse reflection from the walls.

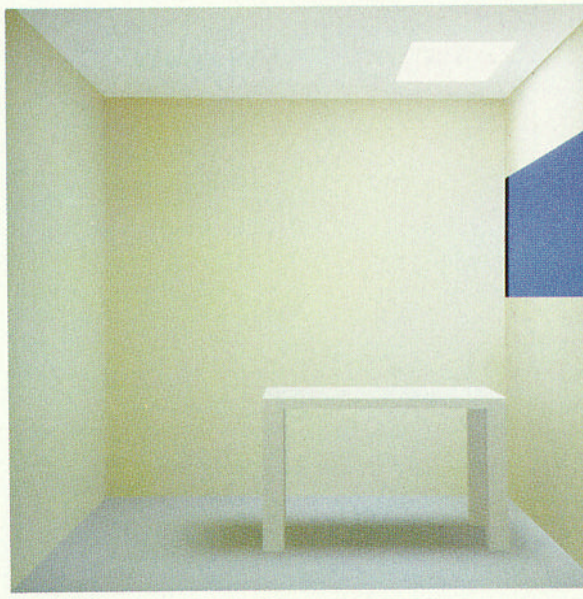

Fig. 10b. Left room in Figure 10a when overhead lights in both rooms are turned on. Light coming in through the blue window has little effect on the appearance of the room.

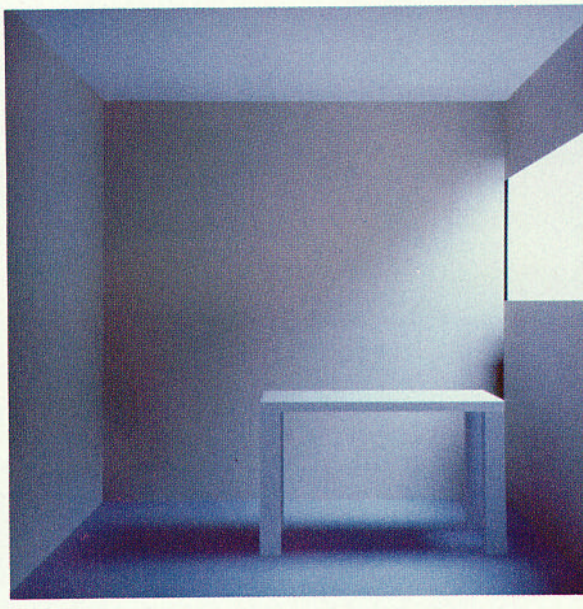

Fig. 10c. Left room in Figure 10a when overhead light in the left room is turned off and overhead light in the right room is turned on. All light in the left room has been specularly transmitted through the blue window.

Fig. 11a. High-intensity lamp shining on a mirror: Overall view of the room.

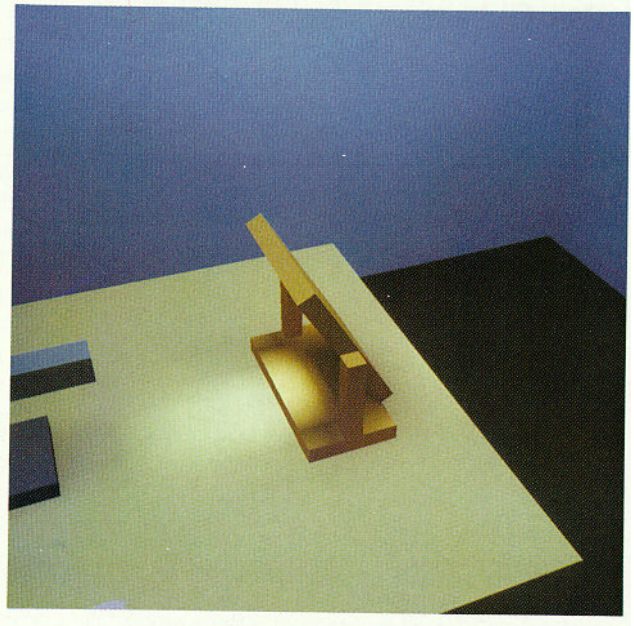

Fig. 11b. High-intensity lamp shining on a mirror: Close-up view of the table surface.

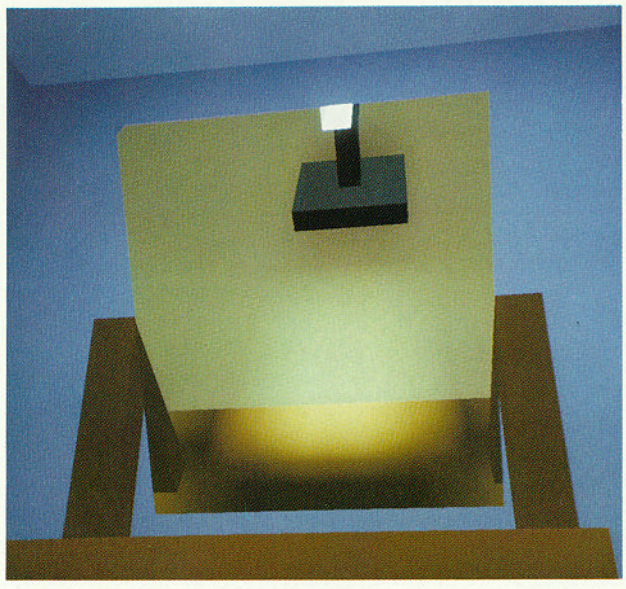

Fig. 11c. High-intensity lamp shining on a mirror: View looking into the mirror.

Figure 10 shows a room under different lighting conditions. The walls of the room are yellow, and the ceiling and table are white. As shown in Figure 10a, the room is adjacent to a similar room on the right. The wall between the rooms has a specularly transmitting blue window. Figure 10b shows the left room when the overhead lights in both rooms are on, whereas Figure 10c shows the left room when the overhead light in the left room is turned off. In Figure 10b the transmitting window has little effect on the appearance of the other surfaces in the room. The transmitted light is of low intensity compared to that received directly from the ceiling light. In Figure 10c the transmitting window has a dramatic effect. All the light in the left room has passed through the window. There is a blue cast in the room, including the ceiling. The ceiling is illuminated by light reflected from the walls and floor of the right room, and then transmitted through the blue window, and by blue light reflected from the table, floor, and walls in the left room. The basic radiosity and ray-tracing methods would incorrectly illuminate the ceiling and other portions of the left room. Those methods do not allow specular transmission/diffuse reflection interactions.

Figure 11 shows three views of a small lamp and mirror sitting on a table in a room. The figure illustrates the reflection of light from a specular surface to a diffuse surface. The lamp is modeled as a diffusely emitting surface recessed in a long square tube. The mirror is modeled as an opaque ideal specularly reflecting surface, All other surfaces are opaque ideal diffuse reflectors. The close-up in Figure 11b shows a bright spot on the table that is the mirror reflection of the small light source. Figure 11c is a view looking into the mirror. The small lamp and the bright spot on the table are visible in the mirror. This image could not

have been constructed with the basic radiosity method, by the ray-tracing method, or by a superposition of the methods.

8. SUMMARY

An extension of the basic radiosity method has been presented. The extended method fully accounts for ideal specular and ideal diffuse reflection, and ideal specular and ideal diffuse transmission. The method is implemented by computing additional form factors using variations of the hemicube method for calculating forward diffuse form factors. The implementation is restricted to environments in which a small number of specular surfaces have a visible impact on the illumination of diffuse surfaces. Images with a translucent lamp shade, a colored window, and a mirror illustrate the application of the method.

The extended radiosity method is used as the first pass in Wallace et al.'s two-pass method [13]. The two-pass method is a practical alternative to the more general, but also more computationally expensive, methods of Immel et al. [7] and Kajiya [8]. Like Immel et al.'s method, the extended radiosity method uses additional form factors to account for the effect of specular surfaces on the illumination of diffuse surfaces. Unlike Immel et al.'s method, the number of additional factors is limited to a few that have a visible impact on the image, and the number of simultaneous equations to be solved has not been increased. In this paper the assumptions behind the extended radiosity method have been discussed with a view to defining the accuracy and utility of the method.

Future efforts to improve the extended radiosity method should include developing a database for actual bidirectional reflectances, expressed as linear combinations of ideal diffuse/ideal specular. Also, a procedure is needed to help determine when specular reflections will have a visible impact on a diffuse surface and to thereby automatically determine when to calculate the additional form factors.

ACKNOWLEDGMENTS

This study is part of a continuing effort in the Program of Computer Graphics at Cornell University to develop physically based lighting models. We are grateful to Professor Donald Greenberg and Professor Michael Cohen for helpful discussions and encouragement during this study. The raster images were photographed by Emil Ghinger.

REFERENCES

1. COHEN, M. F., AND GREENBERG, D. P. The hemi-cube: A radiosity solution for complex environments. In *Proceedings of SIGGRAPH 85* (San Francisco, Calif., July 22–26). *Comput. Graph. 19*, 3 (July 1985), 31–40.
2. COOK, R. L., PORTER, T., AND CARPENTER, L. Distributed ray tracing. In *Proceedings of SIGGRAPH 84* (Minneapolis, Minn., July 23–27). *Comput. Graph. 18*, 3 (July 1984), 137–145.
3. DRISCOLL, W. G., AND VAUGHN, W. *Handbook of Optics*. McGraw-Hill, New York, 1978.
4. DUNKLE, R. V. Radiant interchange in an enclosure with specular surfaces and enclosures with windows or diathermanous walls. In *Heat Transfer, Thermodynamics and Education*, H. A. Johnson, Ed. Boelter Anniversary Volume, McGraw-Hill, New York, 1964.

5. ECKERT, E. R. G., AND SPARROW, E. M. Radiative heat exchange between surfaces with specular reflection. *Int. J. Heat Mass Transfer 3*, 1 (Aug. 1961), 42–54.
6. GORAL, C. M., TORRANCE, K. E., GREENBERG, D. P., AND BATTAILE, B. Modeling the interaction of light between diffuse surfaces. In *Proceedings of SIGGRAPH 84* (Minneapolis, Minn., July 23–27). *Comput. Graph. 18*, 3 (July 1984), 213–222.
7. IMMEL, D. S., COHEN, M. F., AND GREENBERG, D. P. A radiosity method for non-diffuse environments. In *Proceedings of SIGGRAPH 86* (Dallas, Tex., Aug. 18–22). *Comput. Graph. 20*, 4 (Aug. 1986), 133–142.
8. KAJIYA, J. T. The rendering equation. In *Proceedings of SIGGRAPH 86* (Dallas, Tex., Aug. 18–22). *Comput. Graph. 20*, 4 (Aug. 1986), 143–150.
9. NISHITA, T., AND NAKAMAE, E. Continuous tone representation of three dimensional objects taking account of shadows and interreflection. In *Proceedings of SIGGRAPH 85* (San Francisco, Calif., July 22–26). *Comput. Graph. 19*, 3 (July 1985), 23–30.
10. NISHITA, T., AND NAKAMAE, E. Continuous tone representation of three dimensional objects illuminated by sky light. In *Proceedings of SIGGRAPH 86* (Dallas, Tex., Aug. 18–22). *Comput. Graph. 20*, 4 (Aug. 1986), 125–132.
11. RUSHMEIER, H. E. Extending the radiosity method to transmitting and specularly reflecting surfaces. M.S. thesis, Sibley School of Mechanical and Aerospace Engineering, Cornell Univ., Ithaca, N.Y., Jan. 1986.
12. SIEGEL, R., AND HOWELL, J. R. *Thermal Radiation Heat Transfer*. Hemisphere Publishing Corp., Washington, D.C., 1981.
13. WALLACE, J. R., COHEN, M. F., AND GREENBERG, D. P. A two-pass solution to the rendering equation: A synthesis of ray tracing and radiosity methods. In *Proceedings of SIGGRAPH 87* (Anaheim, Calif., July 27–31). *Comput. Graph. 21*, 3 (July 1987), 311–320.
14. WHITTED, T. An improved illumination model for shaded display. *Commun. ACM 23*, 6 (June 1980), 343–349.

Received October 1987; revised May 1988 and August 1988; accepted October 1988

Editor: Loren Carpenter